PREPRINT 499

DECEMBER 2019

Coupling of Linear Elastic Equations and Compressible Euler Equations and Stiffened Gas*

Michael Herty, Siegfried Müller and Aleksey Sikstel

Institut für Geometrie und Praktische Mathematik
Templergraben 55, 52062 Aachen, Germany

Institut für Geometrie und Praktische Mathematik, RWTH Aachen, Templergraben 55, 52056 Aachen, Germany
Michael Herty, email: herty@igpm.rwth-aachen.de
Siegfried Müller, email: mueller@igpm.rwth-aachen.de
Aleksey Sikstel, email: sikstel@igpm.rwth-aachen.de

* This work has been supported in part by the German Research Council (DFG) within the DFG Collaborative Research Center SFB-TR-40, TP A1, and by KI-Net NSF RNMS grant No. 1107444, grants DFG Cluster of Excellence 'Production technologies for high–wage countries', HE5386/13,14,15- 1, DAAD–MIUR project, Deutsche Forschungsgesellschaft HE5386/13,15 and Bundesministerium für Bildung und Forschung 05M18PAA.

Coupling of Linear Elastic Equations and Compressible Euler Equations and Stiffened Gas Equations of State *

Michael Herty, Siegfried Müller and Aleksey Sikstel

Abstract Modelling of cavitation phenomena requires coupling of models for fluid and solid materials. For this purpose we extend a strategy based on the solution of coupled Riemann problems, proposed in [9]. The coupling strategy for the case of perfect gas equation of state has been established and validated in [8]. In this work we include the case of a stiffened gas and derive conditions under which there exists a unique solution to coupled Riemann problems.

Key words: Linear elastic equations, compressible Euler equations, coupling conditions, coupled Riemann problem, Lax curves

1 Introduction

Cavitation erosion is caused in solids exposed to strong pressure waves developing in an adjacent fluid field. The knowledge of the transient distribution of stresses in the

Michael Herty
Institut für Geometrie und Praktische Mathematik, RWTH Aachen, Templergraben 55, 52056 Aachen, Germany, e-mail: herty@igpm.rwth-aachen.de

Siegfried Müller
Institut für Geometrie und Praktische Mathematik, RWTH Aachen, Templergraben 55, 52056 Aachen, Germany, e-mail: mueller@igpm.rwth-aachen.de

Aleksey Sikstel
Institut für Geometrie und Praktische Mathematik, RWTH Aachen, Templergraben 55, 52056 Aachen, Germany, e-mail: sikstel@igpm.rwth-aachen.de

* This work has been supported in part by the German Research Council (DFG) within the DFG Collaborative Research Center SFB-TR-40, TP A1, and by KI-Net NSF RNMS grant No. 1107444, grants DFG Cluster of Excellence 'Production technologies for high–wage countries', HE5386/13,14,15- 1, DAAD–MIUR project, Deutsche Forschungsgesellschaft HE5386/13,15 and Bundesministerium für Bildung und Forschung 05M18PAA.

solid is important to understand the cause of damaging by comparisons to breaking points of the material. The modelling of this problem requires coupling of models for fluid and solid.

This concept has been realised by coupling linear elastic structures and fluids governed by the compressible Euler equations at a steady interface. We refer to this kind of problems as fluid-structure coupling problem (FSC). For a perfect gas equation of state (EoS) the FSC has been solved previously in [8] by means of coupled RPs. This leads in fact to identifying the unique root of a scalar nonlinear function. Properties of this function, and hence, conditions for the existence of a unique solution of the FSC have been presented in Theorem 3.1, [8].

In this work we present a new result, namely the FSC with a stiffened gas EoS. Those EoS are more suitable for fluids such as water. The stiffened gas EoS models the fluid as an ideal gas under high pressure. For that purpose, pressure and internal energy of an ideal gas EoS are scaled. Although the shift from ideal to stiffened gas is linear, the solution of the FSC with stiffened gas EoS may differ drastically from the ideal fluid case due to the *nonlinear* nature of the fluid. Lax curves corresponding to the compressible Euler equations with stiffened gas EoS have to be determined to obtain states at the coupling interface. A scalar nonlinear function is then constructed. Its root provides a unique solution to the FSC. We state similar results and accompanying proofs as in [8].

2 Riemann Problems for Coupled Conservation Laws

Coupling the dynamics requires to postulate conditions to be fulfilled at the interface for almost all times $t \geq 0$. Let the domain Ω be partitioned into two subdomains

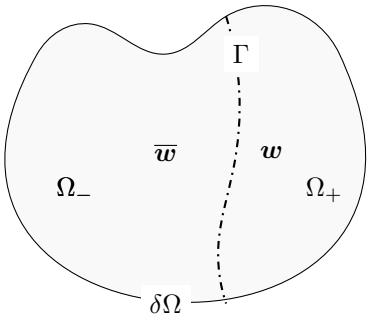

Fig. 1 Domain of the coupled conservation laws.

$\Omega_- \cup \Omega_+ \cup \Gamma = \Omega$ by a fixed interface plane Γ , see Figure 1. Assume that the dynamics in Ω_- are governed by a system of conservation laws

$$\overline{\mathbf{w}}_t + \operatorname{div}(\overline{\mathbf{f}}(\overline{\mathbf{w}})) = 0,\ \mathbf{x} \in \Omega_-,\ t \geq 0, \tag{1}$$

$$\overline{\mathbf{w}}(0, \mathbf{x}) = \overline{\mathbf{w}}_0(\mathbf{x}),\ \mathbf{x} \in \Omega_- \tag{2}$$

for the conserved quantity $\overline{\mathbf{w}}\colon \mathbb{R}_+ \times \Omega_- \to \overline{\mathcal{D}}$ and differentiable flux function $\overline{\mathbf{f}}\colon \overline{\mathcal{D}} \to \mathbb{R}^{\overline{m}}$ where $\overline{\mathcal{D}} \subset \mathbb{R}^{\overline{m}}$ is the set of admissible values for $\overline{\mathbf{w}}$. The dynamics in the other half of the domain, Ω_+, is governed by the system

$$\mathbf{w}_t + \operatorname{div}(\mathbf{f}(\mathbf{w})) = 0,\ \mathbf{x} \in \Omega_+,\ t \geq 0 \tag{3}$$

$$\mathbf{w}(0, \mathbf{x}) = \mathbf{w}_0(\mathbf{x}) \text{ for } \mathbf{x} \in \Omega_+ \tag{4}$$

for $\mathbf{w}\colon \mathbb{R}_+ \times \Omega_+ \to \mathcal{D}$ and a possibly different differentiable flux function $\mathbf{f}\colon \mathcal{D} \to \mathbb{R}^m$ where $\mathcal{D} \subset \mathbb{R}^m$ is the set of admissible values for $\mathbf{w}$. At the non-interface boundary of each domain $\delta\Omega_- \backslash \Gamma$ and $\delta\Omega_+ \backslash \Gamma$ we prescribe boundary conditions, cf. [7]. At the interface Γ we prescribe coupling conditions

$$\boldsymbol{\Psi}\left(\overline{\mathbf{w}}(t, \mathbf{x}), \mathbf{w}(t, \mathbf{x})\right) = 0,\ \mathbf{x} \in \Gamma \tag{5}$$

where $\boldsymbol{\Psi} : \mathbb{R}^{\overline{m}+m} \to \mathbb{R}^{\ell}$. We refer to [2] for a precise definition in the case of a 2×2 system of conservation laws.

Definition 1 Let the domain Ω be separated by a smooth interface Γ, i.e. $\Omega = \Omega_- \cup \Omega_+ \cup \Gamma$, see Figure 1. As a **weak solution of the coupled problem** we understand a pair of weak entropy solutions $(\overline{\mathbf{w}}(t, \mathbf{x}), \mathbf{w}(t, \mathbf{x}))$ to equation (1) and equation (3) for $\mathbf{x} \in \Omega_-$ and $\mathbf{x} \in \Omega_+$, respectively. Further, assuming the traces of $\overline{\mathbf{w}}$ and $\mathbf{w}$ at Γ exist, the solution at $\mathbf{x} \in \Gamma$ fulfils a.e. in t the coupling condition $\boldsymbol{\Psi} = 0$, that is

$$\boldsymbol{\Psi}(\overline{\mathbf{w}}(t, \mathbf{x}^-), \mathbf{w}(t, \mathbf{x}^+)) = 0,\ t > 0,\ \mathbf{x} \in \Gamma, \tag{6}$$

where

$$\begin{aligned} \overline{\mathbf{w}}(\mathbf{x}^-) &:= \lim_{\varepsilon \to 0^+} \overline{\mathbf{w}}(\mathbf{x} - \varepsilon \mathbf{n}), \\ \mathbf{w}(\mathbf{x}^+) &:= \lim_{\varepsilon \to 0^+} \mathbf{w}(\mathbf{x} + \varepsilon \mathbf{n}) \end{aligned} \tag{7}$$

denote the limits in the normal direction $\mathbf{n} = \mathbf{n}(\mathbf{x})$ of Γ.

Remark 1 It is reasonable to assume that whenever $\ell = \overline{m} = m$, $\mathbf{f} = \overline{\mathbf{f}}$ and $\boldsymbol{\Psi}(\overline{\mathbf{v}}, \mathbf{v}) = \overline{\mathbf{f}}(\overline{\mathbf{v}}) - \mathbf{f}(\mathbf{v})$ the solution of the coupling problem coincides with the solution of the single conservation law

$$\mathbf{w}_t + \operatorname{div}(\mathbf{f}(\mathbf{w})) = 0,\ \mathbf{x} \in \Omega,\ t \geq 0, \tag{8}$$

$$\mathbf{w}(0, \mathbf{x}) = \overline{\mathbf{w}}_0(\mathbf{x}),\ \mathbf{x} \in \Omega_-, \tag{9}$$

$$\mathbf{w}(0, \mathbf{x}) = \mathbf{w}_0(\mathbf{x}),\ \mathbf{x} \in \Omega_+. \tag{10}$$

In order to solve the coupled problem (1)–(5) an approach is to iterate the coupling condition at each time step solving alternately the conservation laws (1) and (3) as in [5, 10]. Besides being computationally expensive such methods have significant drawbacks. Firstly, it is in general an open question if and how fast the iterative method for the coupling condition converges. Secondly, given a convergent method there is no guarantee that the limit constitutes an entropy solution in $\Omega_\pm$.

Alternatively, one may use a strategy based on the solution of coupled Riemann Problems (RP) that has been applied and validated e.g. in [1, 8]. To this end, we project the conservation laws (1) and (3) to the normal direction at Γ and define two (half-)RPs that are coupled by conditions $\Psi = 0$ at Γ. A (half-)RP associated with the conservation law (1) on Ω_- consists of the initial data

$$\overline{\mathbf{w}}(0,\mathbf{x}) = \begin{cases} \overline{\mathbf{w}}_L & \text{if } \mathbf{x} \in \Omega_-, \\ \overline{\mathbf{w}}_\Gamma & \text{if } \mathbf{x} \in \Gamma \end{cases} \tag{11}$$

where $\overline{\mathbf{w}}_L$ and $\overline{\mathbf{w}}_\Gamma$ are constant. The solution $\overline{\mathbf{w}} = \overline{\mathbf{w}}(t,\mathbf{x})$ of the (half-)RP is the solution *restricted to* Ω_- of the classical RP for the projected conservation law (1) and initial data (11). Similarly, we consider a (half-)RP associated with the projected conservation law (3) on Ω_+ and initial data

$$\mathbf{w}(0,\mathbf{x}) = \begin{cases} \mathbf{w}_\Gamma & \text{if } \mathbf{x} \in \Gamma, \\ \mathbf{w}_R & \text{if } \mathbf{x} \in \Omega_+ \end{cases} \tag{12}$$

where again $\mathbf{w}_\Gamma$ and $\mathbf{w}_R$ are constant. In view of the coupling problems, particularly interesting are solutions where the trace of the solution in Ω_- fulfils $\overline{\mathbf{w}}(t,\mathbf{x}^-) = \overline{\mathbf{v}}$, and in Ω_+ the trace of the solution fulfils $\mathbf{w}(t,\mathbf{x}^+) = \mathbf{v}$ such that the coupling conditions $\Psi(\overline{\mathbf{v}},\mathbf{v}) = 0$ hold true.

Given a constant state $\overline{\mathbf{w}}_L$ we introduce the notion of admissible boundary states as follows. The set

$$\overline{V}(\overline{\mathbf{w}}_L) := \Bigg\{ \overline{\mathbf{v}} \in \overline{\mathcal{D}} : \ \exists\, (\varepsilon_i)_{i=1}^{\overline{M}} \subset \mathbb{R}^{\overline{M}}, \\ \overline{\mathbf{v}} = \overline{L}_{\overline{M}}^{+}\Big(\varepsilon_{\overline{M}}; \overline{L}_{\overline{M}-1}^{+}\big(\varepsilon_{\overline{M}-1}; \dots; \overline{L}_1^{+}(\varepsilon_1, \overline{\mathbf{w}}_L)\dots\big)\Big) \Bigg\} \tag{13}$$

consists of all states $\overline{\mathbf{v}} = \overline{\mathbf{w}}(t,\mathbf{x}^-)$ that solve a (half-)RP in Ω_-, i.e. are attainable by a composition of forward Lax curves $\overline{L}_{\overline{m}}^{+}(\cdot\,;\,\overline{\mathbf{w}}_0^{\overline{m}})$, $\overline{m} \in \{1,\dots\overline{M}\}$ each emerging at some $\overline{\mathbf{w}}_0^{\overline{m}} \in \overline{\mathcal{D}}$. Furthermore, $\overline{M}$ is chosen such that for the eigenvalues of the Jacobian of the flux $\overline{f}$ in (1) $\overline{\lambda}_{\overline{M}} < 0$ and $\overline{\lambda}_{\overline{M}+1} > 0$ holds. Thus, the $\overline{M}$-th Lax curve $\overline{L}_{\overline{M}}^{+}(\cdot\,;\,\mathbf{w}_0)$ connects $\mathbf{w}_0$ to a state that is located at the interface. Similarly, for a given state $\mathbf{w}_R$ the set of admissible boundary states in Ω_+ is defined by

$$V(\mathbf{w}_R) := \Big\{ \mathbf{v} \in \mathcal{D} : \exists (\theta_i)_{i=1}^{M} \subset \mathbb{R}^M, \\ \mathbf{v} = L_M^-\Big(\theta_M; L_{M-1}^-\big(\theta_{M-1}; \ldots; L_1^-(\theta_1, \mathbf{w}_R)\ldots\big)\Big)\Big\} \quad (14)$$

where M is chosen such that the eigenvalues of the Jacobian of the flux f in (3) $\lambda_M > 0$ and $\lambda_{M-1} < 0$.

Definition 2 Having the sets $\overline{V}(\overline{\mathbf{w}}_L)$ and $V(\mathbf{w}_R)$ at hand the solution to the coupled problem is constructed as follows: we need to prove that there exist unique states $\overline{\mathbf{v}} \in \overline{V}(\overline{\mathbf{w}}_L)$ and $\mathbf{v} \in V(\mathbf{w}_R)$ such that $\boldsymbol{\Psi}(\overline{\mathbf{v}}, \mathbf{v}) = 0$. Provided the traces of the solutions in $\Omega_\pm$ are well-defined and unique $\overline{\mathbf{v}}$ and $\mathbf{v}$ are identified the **solution to the coupled RP** is given by the solution of the two half-RPs with the corresponding initial data $(\overline{\mathbf{w}}_L, \overline{\mathbf{v}})$ and $(\mathbf{v}, \mathbf{w}_R)$, respectively.

By definition of the sets $V(\mathbf{w}_R), \overline{V}(\overline{\mathbf{w}}_L)$, the trace of the solution fulfils the coupling condition. The solution of the coupled RP is summarised in the following algorithm.

Algorithm 1 Riemann Solver for Coupled Problems

1: Let $\mathbf{x} \in \Gamma$ be a point at the interface, $\overline{\mathbf{w}}_L = \overline{\mathbf{w}}(t, \mathbf{x}^-)$ and $\mathbf{w}_R = \mathbf{w}(t, \mathbf{x}^+)$ be the attached interface states for the systems in Ω_- and Ω_+ respectively.
2: Project the systems of conservation laws on the normal interface direction $\mathbf{n} = \mathbf{n}(\mathbf{x})$.
3: Solve the coupled RP consisting of two half-RPs. Thus, identify the sets of admissible boundary states $\overline{V}$ and V by compositions of Lax curves. Find parameters $(\varepsilon_i^*)_{i=1}^{M}$ and $(\theta_i^*)_{i=1}^{M}$ corresponding to $\overline{\mathbf{v}}^* \in \overline{V}(\mathbf{w}_L)$ and $\mathbf{v}^* \in V(\mathbf{w}_R)$, respectively, satisfying $\boldsymbol{\Psi}(\overline{\mathbf{v}}^*, \mathbf{v}^*) = 0$.
4: Evaluate the Lax curves with respect to ε^* and θ^* to determine the boundary values $\overline{\mathbf{w}} = \overline{\mathbf{w}}(\varepsilon^*)$ and $\mathbf{w} = \mathbf{w}(\theta^*)$ for both systems of conservation laws.
5: Project the systems of conservation laws back on $\Omega_\pm$.

3 Fluid-Structure Coupling: Linear Elastic and Compressible Euler Equations

In this section Algorithm 1 is applied to the FSC problem with stiffened gas EoS. After introducing the model for the FSC the sets $\overline{V}$ and V are determined. Finally, the existence of a unique solution of a RP for the FSC is analysed.

3.1 Modelling of the Fluid-Structure Coupling Problem

Consider a situation as sketched in Figure 2 where the interface Γ separates a material and a compressible fluid. It is assumed that the interface remains unaffected by the interaction of the fluid flow with a material structure [5], i.e. we do not account for deformation of the structure. The solid regime and the fluid regime is assumed to be

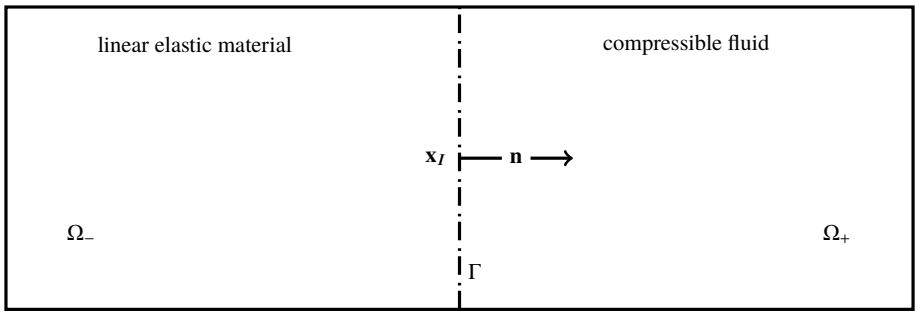

Fig. 2 Sketch of the 2D FSC problem with elastic material on the left and compressible fluid on the right. Shown is the interface Γ (dashed) with its normal direction $\boldsymbol{n}$ starting at $\mathbf{x}_I \in \Gamma$.

governed by the linear elastic equations

$$\frac{\partial \overline{\mathbf{v}}}{\partial t} - \frac{1}{\overline{\rho}} \nabla \cdot \overline{\boldsymbol{\sigma}} = \mathbf{0}, \tag{15a}$$

$$\frac{\partial \overline{\boldsymbol{\sigma}}}{\partial t} - \overline{\lambda} (\nabla \cdot \overline{\mathbf{v}}) \boldsymbol{I} - \overline{\mu} \left(\nabla \overline{\mathbf{v}} + \nabla \overline{\mathbf{v}}^T \right) = \mathbf{0}. \tag{15b}$$

Here, the density of the material is denoted by $\overline{\rho}$ and assumed to be constant. The deformation velocities are $\overline{\mathbf{v}} = (\overline{v}_1, \ldots, \overline{v}_d)^T$, the stress tensor is denoted by $\overline{\boldsymbol{\sigma}} = (\overline{\sigma}_{ij})_{i,j,=1,\ldots,d} = \overline{\boldsymbol{\sigma}}^T$, and the Lamé constants are $\overline{\lambda}$, $\overline{\mu} > 0$. Finally, the dilatation wave velocity and the shear wave velocity are $\overline{c}_1^2 := (2\overline{\mu} + \overline{\lambda})/\overline{\rho}$ and $\overline{c}_2^2 := \overline{\mu}/\overline{\rho}$, respectively. Due to the symmetry of the stress tensor $\overline{\boldsymbol{\sigma}}$, the system of equations (15) contains redundant equations. Those may be removed and the system can be written in the canonical form of a system of conservation laws, see equation (29) in the Appendix A of [8].

The fluid regime is governed by the compressible Euler equations

$$\frac{\partial \rho}{\partial t} + \nabla \cdot (\rho \mathbf{v}) = 0, \tag{16a}$$

$$\frac{\partial \rho \mathbf{v}}{\partial t} + \nabla \cdot (\rho \mathbf{v}^T \mathbf{v} + p \boldsymbol{I}) = \mathbf{0}, \tag{16b}$$

$$\frac{\partial \rho E}{\partial t} + \nabla \cdot (\rho \, \mathbf{v}(E + p/\rho)) = 0, \tag{16c}$$

where we use the notation ρ for the gas density, $\mathbf{v} = (v_1, \ldots, v_d)^T$ for its velocity, E for the total energy $E = e + \frac{1}{2}\mathbf{v}^2$, pressure p, internal energy e and total enthalpy $H := E + \frac{p}{\rho}$. The fluid equations have to be supplemented with an EoS, see [11, 4]. Here, we consider a stiffened gas EoS

$$p(\rho, e) = (\gamma - 1)\rho(e - Q) - \gamma\pi, \tag{17}$$

where γ, Q and π are constants, see for instance [6]. In particular, $\gamma > 1$ denotes the ratio of specific heats at constant pressure, Q is the formation enthalpy and π is referenced to as the pressure stiffness. Setting Q and π to zero results in the ideal gas EoS.

Across the interface we couple the fluid dynamics model (16) to the solid model (15). To this end, we again project the system of equations onto the normal direction $\boldsymbol{n}$ of the interface. For notational convenience we assume the normal direction $\boldsymbol{n}$ pointing from the solid towards the fluid regime, see Figure 2. The projection of the linear elastic model in $d \in \{1, 2, 3\}$ spatial dimensions is realised by means of the matrices $\boldsymbol{R}_d$, $\boldsymbol{S}_d$ and $\boldsymbol{G}_d$, introduced in the Appendix A of [8], to obtain a quasi–1D model in the normal direction. Similarly, we project the fluid equations (16) assuming there is no flow in tangential directions. Since both systems (16) and (15) are invariant under rotation and reflection, it is sufficient to consider the projection onto direction $\boldsymbol{n} = \boldsymbol{e}_1 = (1, 0, \ldots, 0)^T \in \mathbb{R}^d$, as depicted in Figure 2.

The basic problem is now to couple the two projected systems at the interface Γ. Note that the projected linear elastic model is defined in Ω_- and the projected Euler equations in Ω_+. To distinguish the fluid states from the solid states, quantities of the solid shall be denoted by a bar, e.g. $\overline{\mathbf{u}}, \overline{\rho}, \overline{\lambda}$ and so on.

According to the transition conditions of continuum mechanics at a material interface we model the coupling by requiring the following conditions $\Psi = 0$ to be fulfilled at the interface:

$$\boldsymbol{n}^T \overline{\boldsymbol{\sigma}} \boldsymbol{n} \equiv \overline{\sigma}_{nn} \stackrel{!}{=} -p, \tag{18a}$$

$$\overline{\mathbf{v}}^T \boldsymbol{n} \equiv \overline{v}_n \stackrel{!}{=} v_n \equiv \mathbf{v}^T \boldsymbol{n}, \tag{18b}$$

where we neglect viscosity and heat conduction in the fluid flow. The conditions prescribe a continuous normal stress and pressure at the interface. Also, we assume that across the interface the normal velocities are equal. The conditions (18) are referred to as transition and kinematic conditions or coupling conditions, respectively. These conditions are used to provide boundary condition at some point $\mathbf{x}_I \in \Gamma$ of the interface for both the solid and the fluid. The procedure is described in detail in Algorithm 1, and is realised in the following two sections. For both systems the Lax curves are used to prove the existence of a unique solution of the FSC problem provided the initial data in the fluid is subsonic.

3.2 Riemann Problem for the Fluid-Structure Coupling

Solutions of the classical RP for the projected linear elastic and the projected compressible Euler equations are well-known, see [4, 15]. Figure 3 and 4 depict the wave structures for both systems of conservation laws in the x-t plane. According to

Algorithm 1, admissible states for both systems given by respective Lax curves are required.

Definition 3 Let the domain $\Omega = \mathbb{R}^d$, $d \in \{1,2,3\}$, be separated by the interface plane $\Gamma = \{\mathbf{x} \in \mathbb{R}^d : x_1 = 0\}$ into a solid and a fluid subdomain $\Omega_- = \{\mathbf{x} \in \mathbb{R}^d \colon x_1 < 0\}$ and $\Omega_+ = \{\mathbf{x} \in \mathbb{R}^d \colon x_1 > 0\}$. Let the dynamics of the solid and of the fluid be governed by the linear elastic equations (15) and by the compressible Euler equations (16) equipped with stiffened gas EoS (17), respectively. Furthermore, let both systems be projected onto $\mathbf{e}_1$, the normal of Γ. Then, the **FSC Riemann problem** (FSC-RP) is defined by the piecewise constant initial data

$$\boldsymbol{u}(0,\mathbf{x}) = \begin{cases} \overline{\mathbf{u}}_L & \text{if } \mathbf{x} \in \Omega_-, \\ \boldsymbol{u}_R & \text{if } \mathbf{x} \in \Omega_+. \end{cases} \tag{19}$$

First, we consider the solid, i.e. the linear elastic equations. The wave speeds are

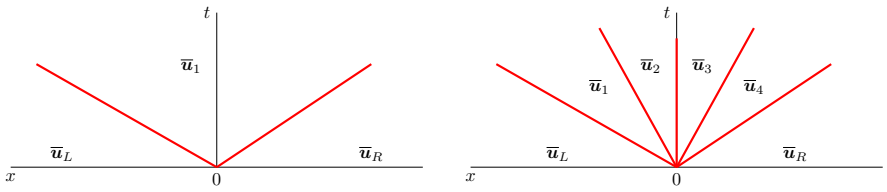

Fig. 3 Wave structure of the linear elastic equations for a classical RP with initial data $\overline{\mathbf{u}}_L, \overline{\mathbf{u}}_R$ where $d = 1$ (left) and $d = 3$ (right).

constant in $\overline{\mathbf{u}}$ and depend on the material parameters of the solid only. Recall that coupled quantities, i.e. normal velocity $\overline{v}_1$ and stress $\overline{\sigma}_{11}$ in the direction $\mathbf{n} = \mathbf{e}_1$, are constant across the waves corresponding to the zero eigenvalue. The admissible states of the solid at Γ are thus obtained by Lax curves $\overline{L}_i(\,\cdot\,;\overline{\mathbf{u}}_L)$, given in [8], emanating from the initial state $\overline{\mathbf{u}}_L$:

$$d = 1 : \ \overline{\mathbf{u}}_1 = \overline{L}_1^+(\varepsilon_1;\overline{\mathbf{u}}_L) = \overline{\mathbf{u}}_L + \varepsilon_1\,\overline{\boldsymbol{r}}_{1,-}, \tag{20a}$$

$$d = 2 : \ \overline{\mathbf{u}}_2 = \overline{L}_2^+(\varepsilon_2;\overline{L}_1^+(\varepsilon_1;\overline{\mathbf{u}}_L)) = \overline{\mathbf{u}}_L + \varepsilon_1\,\overline{\boldsymbol{r}}_{1,-} + \varepsilon_2\,\overline{\boldsymbol{r}}_{2,-}, \tag{20b}$$

$$d = 3 : \ \overline{\mathbf{u}}_2 = \overline{L}_3^+(\varepsilon_3;\overline{L}_2^+(\varepsilon_2;\overline{L}_1^+(\varepsilon_1;\boldsymbol{u}_0))) = \overline{\mathbf{u}}_L + \varepsilon_1\,\overline{\boldsymbol{r}}_{1,-} + \varepsilon_2\,\overline{\boldsymbol{r}}^1_{2,-} + \varepsilon_3\,\overline{\boldsymbol{r}}^2_{2,-}, \tag{20c}$$

where $\overline{\boldsymbol{r}}_{i,-}$ denote the eigenvectors of the flux Jacobian as introduced in the Appendix A of [8] for $d = 1,2,3$.

We investigate the fluid part, i.e. the compressible Euler equations equipped with stiffened gas EoS and subsonic initial data. The wave structure is the same as in the case of a perfect gas EoS. The coupled quantities, i.e. normal velocity and pressure, are constant across the contact wave, however the density may jump. The contact

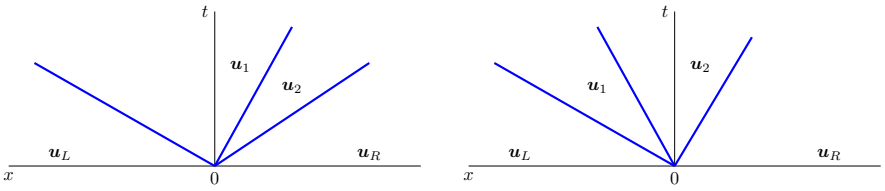

Fig. 4 Wave structure of the compressible Euler equations for a classical RP for subsonic initial data $\mathbf{u}_L, \mathbf{u}_R$ where $\lambda_0 \geq 0$ (left) and $\lambda_0 < 0$ (right).

wave corresponds to the 2-Lax curve, L_2, and the (multiple) flux Jacobian eigenvalue λ_0. In case $\lambda_0 < 0$, admissible fluid states $\mathbf{u}_1$ at Γ are given by the backward 3-Lax curve L_3^- emanating from the initial data $\mathbf{u}_L$. In case $\lambda_0 \geq 0$, the contact wave enters the fluid domain and the composition of L_3^- with the backward 2-Lax curve L_2^- yields the admissible fluid states at Γ, see Figure 4. Thus, admissible interface fluid states $\boldsymbol{u}$ are given by

$$\begin{cases} \mathbf{u}_2 & = \mathbf{L}_3^-(\theta^*; \mathbf{u}_R) \text{ if } \lambda_0 < 0, \\ \mathbf{u}_1 & = \mathbf{L}_2^-(\theta_2; \mathbf{L}_3^-(\theta^*; \mathbf{u}_R)) \text{ if } \lambda_0 \geq 0. \end{cases} \tag{21}$$

In contrast to the solution of the classical RP for the compressible Euler equations, it is not necessary to reparametrise the Lax curves by the pressure. The straightforward parametrisation, as in the definition of Lax curves for the compressible Euler equations [8], suffices for the solution of the FSC-RP.

The following thermodynamic identities are important for the explicit formulation of the 1,3- Lax curves corresponding to genuinely nonlinear waves. The square of the speed of sound, c^2, in terms of density and internal energy reads

$$c^2(\rho, e) = \frac{\gamma(p(\rho, e) + \pi)}{\rho} = \gamma(\gamma - 1)\left(e - Q + \frac{\pi}{\rho}\right). \tag{22}$$

Furthermore, the specific entropy s in terms of density and internal energy

$$s(\rho, e) = c_v \left(\ln\left(\frac{e - Q - \pi/\rho}{c_v}\right) - (\gamma - 1)\ln\rho\right) + Q', \tag{23}$$

where c_v denotes the specific heat at constant volume and Q' is a thermodynamic constant. Finally, internal energy depending on density and specific entropy is given by

$$e(\rho, s) = \exp\left(\frac{s - Q'}{c_v} + (\gamma - 1)\ln\rho\right) + Q + \frac{\pi}{\rho}. \tag{24}$$

For details on the derivation of the above equations, we refer to [6, 14, 12, 3].

Plugging equations (22), (23), (24) and (17) into the general definition of the shock and rarefaction curves for $i = 1, 3$ and applying elementary calculus yields

the 1- and 3-curves for the compressible Euler equations and stiffened gas EoS. The backward (S^-, R^-) and the forward curves (S^+, R^+) read:

$$S_i^{\pm}(\theta, \mathbf{u}_R) = \begin{cases} \rho = \pm(i-2)\theta + \rho_R \\ v = v_R \mp \sqrt{\dfrac{1}{\rho_R}\dfrac{\theta^2\kappa}{\rho(\theta)}\left(\dfrac{2\gamma\rho_R e_R - Q\kappa(2\rho_R \pm (i-2)\theta) - 2\gamma\pi}{2\rho_R \pm (2-i)\kappa\theta} - Q\right)} \\ e = \dfrac{\rho_R}{\rho(\theta)}\dfrac{1}{2 \pm (2-i)\kappa\theta/\rho_R}\Big((2 \pm (i-2)(\gamma+1)\theta/\rho_R)e_R \pm \\ \qquad\qquad (2-i)\theta\dfrac{1}{\rho_R^2}\left(Q\kappa(2\rho_R \pm (i-2)\theta) + 2\gamma\pi\right)\Big) \end{cases}, \tag{25}$$

$$R_i^{\pm}(\theta, \mathbf{u}_R) = \begin{cases} \rho = \pm(i-2)\theta + \rho_R \\ v = v_R + 2(2-i)\sqrt{\dfrac{\gamma}{\gamma-1}}\left(1 - \left(\dfrac{\rho(\theta)}{\rho_R}\right)^{(\gamma-1)/2}\right)\sqrt{e_R - \left(Q + \dfrac{\pi}{\rho_R}\right)} \\ s = s_R \end{cases}, \tag{26}$$

and we have

$$L_I^{\pm} = \begin{cases} S_i^{\pm} & \text{if } \theta < 0 \\ R_i^{\pm} & \text{if } \theta \geq 0 \end{cases}. \tag{27}$$

In the following we assume the initial data is subsonic, i.e.

$$-c(\rho_R, e_R) \leq v_R \leq c(\rho_R, e_R). \tag{28}$$

The wave structure of the FSC-RP is illustrated in Figure 5. The initial data and related quantities are marked with a subscript $_L$ and $_R$ in the solid and fluid part respectively. The admissible fluid states (25), (26) and solid states (20) are used in

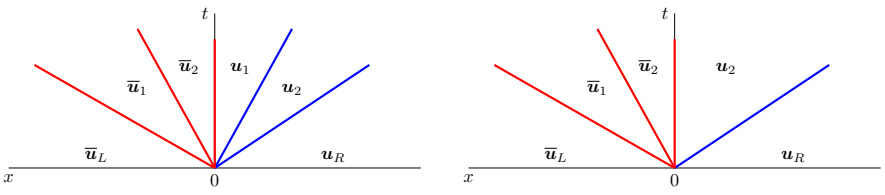

Fig. 5 Wave structure of the FSC-RP for $d \geq 2$ where $\lambda_0 \geq 0$ (left) and $\lambda_0 < 0$ (right). Blue and red lines signify the fluid and solid characteristics respectively.

the coupling conditions (18) with $\mathbf{n} = \mathbf{e}_1$. Then, the coupling conditions (18) depend on the two parameters $\varepsilon := \varepsilon_1 - \overline{\lambda}_1$ and θ

$$\overline{\sigma}_{11}(\varepsilon) \stackrel{!}{=} -p(\theta), \quad \overline{v}_1(\varepsilon) \stackrel{!}{=} v_1(\theta). \tag{29}$$

These are equivalent to

$$\overline{\sigma}_{11,L} + \varepsilon\overline{\rho c}_1\overline{\beta} = -p_3^-(\theta, \mathbf{u}_R), \tag{30a}$$
$$\overline{v}_{1,L} + \varepsilon\overline{\beta} = (v_1)_3^-(\theta, \mathbf{u}_R), \tag{30b}$$

where $\overline{\beta}$ is defined in the Appendix A of [8] for $d = 1, 2, 3$. Hence, the solution of the FSC-RP is equivalent to finding a tuple $(\varepsilon^*, \theta^*)$ that fulfils (30). This is equivalent to

$$g(\theta) := \overline{\sigma}_{11,L} + (v_1(\theta; \mathbf{u}_R) - \overline{v}_{1,L})\overline{\rho c}_1 + p_3^-(\theta; \mathbf{u}_R) = 0, \tag{31a}$$
$$\varepsilon = v_1(\theta; \mathbf{u}_R) - \overline{v}_{1,L}. \tag{31b}$$

Since g does not depend on the parameter ε related to the solid part, it is sufficient to determine the roots of g. This is done in the same manner as for the perfect gas case in [8]. The function g is expressed only in terms of the initial data as follows. For the shock branch, i.e. $\theta \leq 0$, g reads

$$\begin{aligned} g(\theta) = \overline{\sigma}_{11,L} + \overline{\rho c}\left(v_R + \sqrt{\frac{2}{(2\rho_R + (\gamma-1)\theta)(\rho_R - \theta)}}|\theta|c_R - \overline{v}_{1,L}\right) \\ + \frac{1}{\gamma}\frac{2\rho_R - (\gamma+1)\theta}{2\rho_R + (\gamma-1)\theta}\rho_R c_R^2 - \pi, \end{aligned} \tag{32}$$

while for the rarefaction branch, i.e. $\theta \geq 0$,

$$\begin{aligned} g(\theta) = \overline{\sigma}_{11,L} + \overline{\rho c}_1\left(v_R - \frac{2}{\gamma-1}\left(1 - \left(1 - \frac{\theta}{\rho_R}\right)^{\frac{\gamma-1}{2}}\right)c_R - \overline{v}_{1,L}\right) \\ + (\gamma-1)\exp\left(\frac{s_R - Q'}{c_v}\right)(\rho_R - \theta)^\gamma - \pi. \end{aligned} \tag{33}$$

The structure of the solution of $g(\theta) = 0$ will be detailed below.

3.3 Entropy Solutions of the Riemann Problem for the Fluid-Structure Coupling

We investigate properties of the scalar, nonlinear function g to conclude on the existence of its roots and, equivalently, on the solution of the FSC-RP. Statements and proofs are very similar to those given in [8] for the perfect gas case. However, for the sake of completeness and in order to show the behaviour of g for the implementation of the FSC-RP, the following proofs are given at full length.

Lemma 1 *Let $\gamma > 1$, $\rho_R, \overline{\rho}, \overline{c}_1 > 0$ and $p > -\pi$. Then there exist $\theta_m < 0$ and $\theta_M > 0$ such that the function $g : (\theta_m, \theta_M] \to \mathbb{R}$ composed of a shock branch* (32) *and a rarefaction branch* (33) *for $\theta \leq 0$ and $\theta \geq 0$, respectively, is differentiable and strictly monotonically decreasing.*

Proof The shock branch ($\theta \leq 0$) is well-defined provided the discriminant in (33) is positive, i.e.

$$\theta_m := -\frac{2\rho_R}{\gamma - 1} < 0.$$

The rarefaction branch ($\theta \geq 0$) is well-defined provided that the term $(\rho_R - \theta)^{\frac{\gamma-1}{2}}$ is well-defined. Here, two cases have to be distinguished:

$$\theta_M := \begin{cases} \infty & \text{if } \frac{\gamma-1}{2} \in \mathbb{N}, \\ \rho_R & \text{if } \frac{\gamma-1}{2} \in (0, \infty] \backslash \mathbb{N} \end{cases}.$$

The derivatives of g for the shock branch $\theta_m < \theta \leq 0$ and the rarefaction branch $0 \leq \theta \leq \theta_M$ read:

$$g'(\theta) = \bar{\rho}\bar{c}_1\sqrt{2}c\left(\frac{(\gamma-3)\rho_R\theta - 2(\gamma-1)\theta^2}{2[(2\rho_R + (\gamma-1)\theta)(\rho_R - \theta)]^{\frac{3}{2}}} - \frac{1}{\sqrt{(2\rho_R + (\gamma-1)\theta)(\rho_R - \theta)}}\right) - \frac{4\rho^2c^2}{(2\rho + (\gamma-1)\theta)^2}, \quad \theta \leq 0, \tag{34a}$$

$$g'(\theta) = -\frac{\bar{\rho}\bar{c}_1 c}{\rho_R}\left(1 - \frac{\theta}{\rho_R}\right)^{\frac{\gamma-3}{2}} - c^2\left(1 - \frac{\theta}{\rho_R}\right)^{\gamma-1}, \quad \theta \geq 0. \tag{34b}$$

Since the limits at $\theta = 0$ fulfil

$$\begin{aligned} g(0^-) = g(0^+) &= \bar{\sigma}_{11,L} + \bar{\rho}\bar{c}_1\left(v - \bar{v}_{1,L}\right) + \rho c^2/\gamma - \pi, \\ g'(0^-) = g'(0^+) &= -\left(\bar{\rho}\bar{c}_1 + \rho c\right)c/\rho < 0 \end{aligned}$$

and the Lax curves are smooth functions of the parameters, g is continuously differentiable at $\theta = 0$. Next, we show that along the shock branch ($\theta_m < \theta \leq 0$) the function g is strictly monotonically decreasing. According to (34a) this holds true if the inequality

$$(\gamma-3)\rho\theta - 2(\gamma-1)\theta^2 - 2(2\rho + (\gamma-1)\theta)(\rho - \theta) \leq 2\sqrt{2}\frac{\rho^2 c}{\bar{\rho}\bar{c}_1}\sqrt{\frac{(\rho-\theta)^3}{2\rho + (\gamma-1)\theta}}$$

holds. The left-hand side of the inequality reduces to $-\rho(4\rho + \theta(\gamma-3))$ that is negative for $\theta_m < \theta \leq 0$, since

$$\begin{cases} 4\rho + \theta(\gamma-3) \geq 4\rho > 0 & \text{if } 1 < \gamma < 3, \\ 2\rho(\gamma+1)/(\gamma-1) > 0 & \text{if } \gamma \geq 3 \end{cases}.$$

Along the rarefaction branch ($0 \leq \theta \leq \theta_M$) we obtain from (34b)

$$g'(\theta) = -c^2\rho^{-2r}\left(A(\rho-\theta)^{r-1} + (\rho-\theta)^{2r}\right),$$

where $A := c^{-1}\rho^r\bar{\rho}\bar{c}_1 > 0$ and $r := \frac{\gamma-1}{2}$. It is obvious that g' has a single root in ρ. If $r \notin \mathbb{N}$ or $r \in \mathbb{N}$ is odd, then g' is negative for $\theta \in [0, \theta_M)$. If $r \in \mathbb{N}$ is even, then g' is positive if

$$\rho < \theta < \rho + A^{\frac{1}{r+1}}.$$

Therefore, g is strictly monotonically decreasing, if θ does not exceed θ_M. This concludes the proof. □

Since $g \in C^1((\theta_m, \theta_M])$ and g is strictly monotone there exists a unique root of g if g has opposite signs at θ_m and θ_M. This is shown in the next theorem that is equivalent to Theorem 3.1 in [8].

Theorem 1 *Let $\gamma > 1$ and $\rho_R, \overline{\rho}, \overline{c}_1 > 0$, $p_R > -\pi$. The initial data $(\overline{v}_{1,L}, \overline{\sigma}_{11,L})$ and (ρ_R, v_R, p_R) are assumed to satisfy*

$$v_R \leq \frac{2}{\gamma-1}c_R + \overline{v}_{1,L} - \frac{\overline{\sigma}_{11,L}}{\overline{\rho c}_1} + \pi. \tag{35}$$

Then there exists a unique root $\theta^* \in (\theta_m, \theta_M]$ of the function $g : (\theta_m, \theta_M] \to \mathbb{R}$ and therefore a unique solution of the FSC-RP.

Proof For $\theta \leq 0$ we have by definition of g on the shock branch (32)

$$\lim_{\theta \to \theta_m} g(\theta) = \infty.$$

If $\theta \geq 0$ and either $(\gamma-1)/2 \in (0,\infty]\backslash\mathbb{N}$ or $(\gamma-1)/2 \in \mathbb{N}$ even then $\theta_M = \rho_R$ and $g(\theta_M) \leq 0$ provided that

$$\overline{\sigma}_{11,L} + \overline{\rho c}_1\left(v_r - \frac{2}{\gamma-1}c_R - \overline{v}_{1,L}\right) \leq \pi$$

holds. This inequality is satisfied by assumption (35). If $\frac{\gamma-1}{2} \in \mathbb{N}$ is odd then $\theta_M = \infty$ and $\lim_{\theta\to\theta_M} g(\theta) = -\infty$. According to Lemma 1 g is strictly monotonically decreasing in the interval $(\theta_m, \theta_M]$. Thus, by inspecting all cases of limits of g towards the domain θ_m and θ_M the assertion is proven. □

Remark 2 Note that the fluid portion of condition (35) corresponds to the right hand side of the vacuum condition for the classical RP, cf. [15].

4 Conclusions

Condition (35) on the initial data demanded in the previous theorem may be rewritten using the fact that the initial data are subsonic (28).

Lemma 2 *Let $\gamma \in (1,3)$, $\rho_R, \overline{\rho}, \overline{c}_1 > 0$, $p_R > -\pi$ and the initial data in the fluid part be subsonic, i.e. equation* (28) *holds. Then*

$$\overline{v}_{1,L} \geq \frac{\overline{\sigma}_{11,L}}{\overline{\rho c}_1} - \pi \tag{36}$$

is a sufficient condition for a unique solution of the RP for the FSC.

Proof The subsonic condition (28) implies

$$v_R \leq c_R < c_R \frac{2}{\gamma - 1}.$$

Thus, with (36) condition (35) is satisfied. □

We have derived a strategy for the FSC problem employing half-RPs and have shown that under reasonable conditions on the subsonic flow there exists a unique solution of the FSC-RP. This strategy is applied in the coarse of numerical investigations of a bubble collapse, see [13].

References

1. R. M. Colombo and M. Garavello. On the cauchy problem for the p-system at a junction. *SIAM J. Math. Anal.*, 39(5):1456–1471, Jan. 2008.
2. R. M. Colombo, M. Herty, and V. Sachers. On 2×2 conservation laws at a junction. *SIAM J. Math. Anal.*, 40(2):605–622, 2008.
3. R. Courant and K. O. Friedrichs. *Supersonic Flow and Shock Waves*. Applied Mathematical Sciences. Springer New York, 1976.
4. C. M. Dafermos. *Hyperbolic conservation laws in continuum physics*, volume 325 of *Grundlehren der Mathematischen Wissenschaften [Fundamental Principles of Mathematical Sciences]*. Springer-Verlag, Berlin, second edition, 2005.
5. C. Dickopp, R. Gartz, and S. Müller. Coupling of elastic solids with compressible two-phase fluids for the numerical investigation of cavitation damaging. *International Journal on Finite Volumes*, 10:1–39, 2013. hal-01121991.
6. T. Flåtten, A. Morin, and S. T. Munkejord. On solutions to equilibrium problems for systems of stiffened gases. *SIAM Journal on Applied Mathematics*, 71(1):41–67, Jan 2011.
7. E. Godlewski and P.-A. Raviart. *Numerical Approximation of Hyperbolic Systems of Conservation Laws*. Applied Mathematical Sciences. Springer-Verlag, 1996.
8. M. Herty, S. Müller, N. Gerhard, G. Xiang, and B. Wang. Fluid-structure coupling of linear elastic model with compressible flow models. *Int. J. Numer. Methods Fluids*, 86(6):365–391, 2018.
9. M. Herty, S. Müller, and A. Sikstel. Coupling of compressible Euler equations. *Vietnam Journal of Mathematics*, pages 1–24, 2019.

10. G. Hou, J. Wang, and A. Layton. Numerical methods for fluid-structure interaction — a review. *Communications in Computational Physics*, 12(2):337–377, Aug 2012.
11. R. Menikoff and B. Plohr. The Riemann problem for fluid flows of real materials. *Rev. Mod. Phys.*, 61:75–130, 1989.
12. B. J. Plohr. Shockless acceleration of thin plates modeled by a tracked random choice method. *AIAA Journal*, 26(4):470–478, Apr 1988.
13. A. Sikstel. *Analysis and Numerical Methods for the Coupling of Hyperbolic Problems*. PhD thesis, RWTH Aachen University, to appear in 2020.
14. F. Thein. *Results for Two Phase Flows with Phase Transition*. PhD thesis, Universität Magdeburg, 2019.
15. E. F. Toro. *Riemann Solvers and Numerical Methods for Fluid Dynamics: A Practical Introduction*. Springer, 3 edition, 2009.